Morphology, morphogenesis and phylogeny of the new soil ciliate, *Bistichella granulifera* n. sp. (Protista, Ciliophora)

Zhao Lyu
Northwest University
Jingbao Li
Northwestern Polytechnical University
Yurui Wang
Shaanxi Normal University
Jiyang Ma
Shaanxi Normal University
Chen Shao (shaochen@snnu.edu.cn)
Shanxi Normal University https://orcid.org/0000-0001-8474-3204

Research article

Keywords: Bistichella, Novel species, Ontogeny, Phylogenetic, SSU rDNA

Posted Date: August 28th, 2020

DOI: https://doi.org/10.21203/rs.3.rs-48003/v1

Abstract

Background: Hypotrichous ciliates are showing extremely morphological diverse and complicated morphogenesis. However, many hypotrichs are still unknown/poorly-known and need to be explored. Recently, Foissner (2016) reassigned the species in *Bistichella* and *Parabistichella*. Due to lack of morphological and morphogenetic information, some problems were overlooked. In present work, a new species, *Bistichella granulifera* n. sp., was found in northern China. Based on its infraciliature, ontogenesis analyses and phylogenetic study, the phylogenetic position of *Bistichella* was discussed.

Results: *Bistichella granulifera* n. sp. was characterized by having elongated oval body, two macronuclear nodules, cortical granules present, three frontal and three or four buccal cirri, three frontal rows with seven to ten cirri, usually two frontoventral rows with the left one usually terminates at 90% down length of body and no breaks in the right one. The main morphogenetic features of the novel species were as follows: (1) the posterior part of the old adoral membranelles is renewed; (2) frontoventral-transverse cirral anlagen III to V each form a frontal row, and anlagen VI to n each produce a frontoventral row; (3) both marginal rows and dorsal kineties develop intrakinetally; (4) the macronuclear nodules fuse to form a single mass. The gene sequence of *Bistichella* was investigated for the first time. Phylogenetic analyses based on the SSU rDNA sequences showed that the *Bistichella* groups with the non-dorsomarginalian hypotrichs.

Conclusions: Morphology, morphogenesis and phylogenetic position of *Bistichella granulifera* n. sp., was investigated. Each frontoventral row originates from one anlage and only three bipolar dorsal kineties are present in the new species, which means it should belong to non-Dorsomarginalia rather than Amphisiellidae. Even though *Bistichella* has a close relationship with amphisiellids, due to the limited gene sequence, the phylogenetic position of *Bistichella* needs more data to be fully understood.

Background

Hypotrichous ciliates are a highly differentiated group within ciliated protists, and have diversified morphological features and complicated morphogenetic processes [1–8]. To date, many studies have been carried out on the classification and phylogeny of hypotrichs [9–14].

The genus *Bistichella* was originally established by Berger (2008) [1]. Later, mainly due to the presence or absence of transverse cirri, Foissner (2016) [4] reorganized the species in *Bistichella* and *Parabistichella*, and amended the diagnosis of *Bistichella* as follows: two or three short frontal cirral rows and two or three long frontoventral cirral rows, three or four enlarged frontal cirri, more than one buccal cirrus, dorsal kineties in a *Gonostomum*-pattern, transverse cirri and caudal cirri lacking [4]. To date, four species have been assigned to *Bistichella*, namely *B. buitkampi* (Foissner, 1982) Berger, 2008 (type species), *B. humicola* (Gellért, 1956) Berger, 2008, *B. chilensis* Foissner, 2016, and *B. kenyaensis* Foissner, 2016 [1, 4, 15, 16]. However, morphogenetic data in *Bistichella* is still lacking and the gene sequence is unknown.

In this work, a novel soil ciliate *Bistichella granulifera* n. sp. was isolated from Jiangjunshan ancient town, Xi'an, northern China. Observations of its morphology and morphogenetic characteristics demonstrate that it represents a new member of the genus *Bistichella*. The phylogenetic position of *Bistichella* was also investigated.

Results

Zoobank registration.

Present work: urn:lsid:zoobank.org:pub:8AFC5FAA-C4F5-4956-8FFD-41AC2A0C60BF

***Bistichella granulifera* n. sp.**

Zoobank registration.

Bistichella granulifera n. sp.: urn:lsid:zoobank.org:act:4F8D4B63-63DB-41D7-B06F-8E22FD5F68E5

Diagnosis. Size about 110–160 × 40–60 μm *in vivo*. Body elongate oval. Two macronuclear nodules. Single contractile vacuole located near mid-left of body. Cortical granules colourless, about 1 μm across, densely scattered throughout cell surface. 33–38 adoral membranelles, three enlarged frontal cirri and three or four buccal cirri arranged in a row. Three frontal rows, composed about

three cirri in each. Two to four frontoventral rows extending to the posterior of the body. 38–48 and left and 48–54 right marginal cirri. Three bipolar dorsal kineties. Soil habitat.

Type slides. The protargol slide with the holotype specimen (accession number: LZ2016041701A) and another two paratype slides (accession number: LZ2016041701B, C) have been deposited in the Laboratory of Protozoological Biodiversity and Evolution in Wetland, Shaanxi Normal University, China. The holotype specimen (Fig. 1g, h and Fig. 2j, k) was marked on the back of the slide [17, 18].

Type locality. Soil in Jiangjunshan ancient town (34°02'16"N; 109°04'53"E), Xi'an, China.

Etymology. The species-group name '*granulifera*' refers to having cortical granules, which is a main feature of the species. Female gender.

Morphology of *Bistichella granulifera* n. sp. (Fig. 1 and Fig. 2; Table 1)

Table 1 Morphometric characterization of *Bistichella granulifera* n. sp. based on protargol-stained specimens (measurements in µm).

Character	HT	Min	Max	Med	Mean	SD	CV	n
Body, length	128	117	179	136	141	19.69	14	10
Body, width	51	45	68	52	55	8.05	15	10
Body length:width ratio	2.51	2.02	2.96	2.64	2.58	0.32	12	10
AZM, length	41	36	53	44	44	5.45	12	10
AZM/body length	0.32	0.28	0.33	0.32	0.31	0.02	5	10
DE-value	0.21	0.19	0.28	0.24	0.24	0.03	13	10
Number of adoral membranelles	33	33	38	36	35	1.51	4	10
Number of enlarged frontal cirri	3	3	3	3	3	0	0	10
Number of buccal cirri	3	3	4	3	3	0.52	17	10
Number of frontal rows	3	3	3	3	3	0	0	10
Number of cirri in frontal row I	3	2	3	3	3	0.52	17	10
Number of cirri in frontal row II	3	2	3	3	3	0.32	11	10
Number of cirri in frontal row III	4	3	4	4	4	0.48	12	10
Number of frontoventral rows	2	2	4	2	2	0.62	21	10
Number of cirri in frontoventral row I	32	26	37	31	31	3.78	12	10
Number of cirri in frontoventral row II	40	14	44	29	29	10.82	37	10
Number of cirri in frontoventral row III	-	21	41	35	32	-	-	5
Number of cirri in frontoventral row IV	-	21	29	25	25	-	-	2
Number of cirri in left marginal row	44	38	48	46	45	3.36	7	10
Number of cirri in right marginal row	48	48	54	49	50	2.27	5	10
Number of dorsal kineties	3	3	3	3	3	0	0	10
Number of dikinetids in dorsal kinety 1	25	24	30	26	27	2.01	8	10
Number of dikinetids in dorsal kinety 2	24	24	27	26	26	1.16	4	10
Number of dikinetids in dorsal kinety 3	25	25	29	27	27	1.35	5	10
Number of macronuclear nodules	2	2	2	2	2	0	0	10
Length of anterior macronuclear nodule	26	26	44	30	31	5.95	20	10
Width of anterior macronuclear nodule	9	8	16	11	11	2.75	26	10
Number of micronuclei	2	2	3	2	2	0.32	16	10
Diameter of micronuclei	3	3	4	3	3	0.32	11	10

Abbreviations: AZM, adoral zone of membranelles; CV, coefficient of variation in %; for the DE-value, see Berger (2006) for explanation; DK, dorsal kineties; HT, holotype specimen (also included in the sample n); Max, maximum; Mean, arithmetic mean; Med, median value; Min, minimum; n, number of specimens; SD, standard deviation.

Size was 110–160 × 40–60 µm *in vivo* (*n*=5), about 141 × 55 µm on average in protargol impregnation with a ratio of length to width about 2.6:1. Body elongated oval with anterior and posterior ends narrowly and widely rounded respectively, both margins slightly convex, flexible and not contractile (Fig. 1a, g, h and Fig. 2a–c, j, k). Constantly two ellipsoidal macronuclear nodules, about 31 × 11 µm after protargol impregnation, arranged slightly left of the midline (Fig. 1h and Fig. 2h, j). About two globular micronuclei, located near the macronuclear nodules. Contractile vacuole located slightly ahead of mid-body near left margin, about 18 µm across when fully extended (Fig. 1a). Cortical granules densely scattered throughout cell surface, about 1 µm in diameter without colour, (Fig. 1b

and Fig. 2e). Cytoplasm transparent to grayish, contains many lipid droplets, refractive globules and food vacuoles containing small ciliates and bacteria (Fig. 1a and Fig. 2d, i). Locomotion by slowly crawling on substrate or swimming by rotating around the longitudinal axis.

Adoral zone occupied about 31% of the cell length with the distal end extending to the right side; composed 33–38 membranelles, (Fig. 1g and Fig. 2f); largest base of membranelles about 8–15 μm long, cilia about 18 μm long *in vivo*. Paroral and endoral curved anteriorly, and intersect optically near 1/3 to middle of buccal area (Fig. 1g and Fig. 2f, j).

Consistently three enlarged frontal cirri with cilia about 15 μm long *in vivo*. Three to four buccal cirri arranged in a longitudinal row right of the paroral. Three frontal rows, about three or four cirri in each. Frontal rows I and II located at the same level as the buccal cirral row, while frontal row III was a little behind and extends nearly to the proximal end of the adoral zone (Fig. 1g and Fig. 2f). Half of investigated specimens have two frontoventral rows, which are composed of 28–37 and 32–44 cirri. Frontoventral row I started from the level of mid-buccal area, extending slightly obliquely to about 90% of body length. Frontoventral row II started near the anterior end of the distal end of the adoral zone of membranelles (AZM), terminating at the same level as frontoventral row I (Fig. 1g). It is noteworthy that the patterns of frontoventral rows are rather variable in these specimens. In five out of ten individuals, one or two extra frontoventral rows present, short or long (Fig. 1c–f). One left and one right marginal row composed of 38–48 and 48–54 cirri, respectively, not confluent posteriorly (Fig. 1g and Fig. 2j).

Constantly three bipolar dorsal kineties with about 27 dikinetids in each row; dorsal cilia about 3 μm long in life (Fig. 1h and Fig. 2g, k). Caudal cirri lacking.

Morphogenesis (Fig. 3 and Fig. 4)

Only four dividers in different stages of morphogenesis during binary fission were found and the main morphogenetic features are described as follows:

Stomatogenesis and frontoventral-transverse cirral anlagen. In the early divider, the oral primordium are differentiated from anterior to posteriad to form new adoral membranelles in the opisthe; two sets of frontoventral-transverse cirral anlagen are recognizable, and the old frontal and frontoventral rows contribute to the anlagen (Fig. 3a and Fig. 4a). The undulating membranes anlage (UM-anlage = anlage I) appears in each daughter cell (Fig. 3a). The posterior portion of the old AZM is renewed (Fig. 3a and Fig. 4b).

Later, in the middle divider, the new adoral membranelles continue to differentiate in the opisthe, and the leftmost frontal cirrus is derived from the anterior end of anlage I in both dividers (Fig. 3c and Fig. 4d). The proximal membranelles of the old AZM are replaced by new membranelles (Fig. 3c, e and Fig. 4d). All cirral anlagen begin to fragmentize and develop into new cirri (Fig. 3e and Fig. 4f). The cirrus from anlage I together with the anterior-most cirri from anlagen II and III form the three enlarged frontal cirri. A row of buccal cirri is derived from anlage II and migrates near to the new paroral. Cirri from anlagen III to V form three frontal rows, and anlagen VI to n each produces a frontoventral row. Also, additional anlagen are present, which may contribute the additional long or short ventral rows (Fig. 3c, e, g and Fig. 4d, f).

In a late divider, the differentiation of membranelles is completed, and the anterior end of the newly AZM bends to the right in the opisthe. The UM-anlage splits longitudinally to form the paroral and endoral. The new cirri migrate to their final positions and replace the parental structures (Fig. 3g and Fig. 4g).

Development of marginal rows and dorsal kineties. The formation of the marginal rows and dorsal kineties proceeds intrakinetally that some old cirri within each parental row dedifferentiate and form the anlagen. These anlagen then stretch longitudinally and replace the parental structures completely (Fig. 3a–h and Fig. 4a, c, g, h).

Division of nuclear apparatus. Two macronuclear nodules fuse to form a single mass during the middle stage and then divide to form two nodules for both dividers. Micronuclei divide mitotically (Fig. 3b, d, f, h and Fig. 4e).

Phylogenetic analyses based on SSU rDNA sequences (Fig. 5)

The length and GC content of the SSU rDNA sequence of *Bistichella granulifera* n. sp. (GenBank accession number: MT604042) are 1676 bp and 46.12%, respectively. Phylogenetic trees were inferred from the SSU rDNA sequences using two different methods (ML

and BI), and the topologies of two trees were basically congruent. Therefore, only the ML tree with bootstraps and posterior probabilities from both algorithms is presented (Fig. 5).

In the phylogenetic trees, *Bistichella granulifera* n. sp. forms a large clade with species in the genera *Uroleptoides*, *Parabistichella*, *Orthoamphisiella*, *Lamtostyla*, *Keronopsis*, *Paraholosticha* and *Pseudokahliella* with low support (14% ML, 0.32 BI). The sequence similarity between *B. granulifera* n. sp. and the species in this clade ranges from 92.1% to 99.1% (Table 2).

Table 2 Percentages of sequence identity (lower left) and pairwise distance (upper right) based on SSU rDNA sequences between *Bistichella granulifera* n. sp. and the species which formed a big clade with the new species in Fig. 5.

Species	1	2	3	4	5	6	7	8	9	10	11	12	13	14	15	16
1 *Uroleptoides magnigranulosus* AM412774		0.000	0.000	0.001	0.003	0.003	0.002	0.001	0.002	0.002	0.003	0.003	0.003	0.004	0.009	0.020
2 *Uroleptoides longiseries* MH143251	0.968		0.000	0.001	0.003	0.003	0.002	0.001	0.002	0.002	0.003	0.003	0.003	0.004	0.009	0.020
3 *Parabistichella multilineae* MK265247	0.888	0.916		0.001	0.003	0.003	0.002	0.001	0.002	0.002	0.003	0.003	0.003	0.004	0.009	0.020
4 *Parabistichella variabilis* JN008943	0.998	0.968	0.887		0.005	0.005	0.003	0.003	0.003	0.002	0.005	0.005	0.004	0.005	0.009	0.020
5 *Orthoamphisiella breviseries* AY498654	0.996	0.966	0.886	0.995		0.003	0.003	0.002	0.001	0.003	0.004	0.004	0.003	0.002	0.007	0.017
6 *Orthoamphisiella namibiense* JQ723974	0.993	0.962	0.885	0.992	0.994		0.003	0.002	0.001	0.003	0.004	0.004	0.003	0.003	0.008	0.020
7 *Bistichella granulifera* n. sp. MT604042	0.960	0.954	0.921	0.959	0.960	0.956		0.001	0.001	0.001	0.003	0.003	0.002	0.003	0.008	0.018
8 *Lamtostyla salina* KX641150	0.968	0.962	0.915	0.967	0.968	0.964	0.988		0.001	0.001	0.002	0.002	0.001	0.003	0.008	0.019
9 *Keronopsis helluo* KY492516	0.927	0.930	0.953	0.927	0.928	0.925	0.965	0.955		0.001	0.003	0.003	0.002	0.002	0.007	0.018
10 *Paraholosticha pannonica* KY492517	0.927	0.930	0.953	0.928	0.927	0.924	0.965	0.955	0.998		0.003	0.003	0.002	0.003	0.007	0.020
11 *Parabistichella xui* HQ699895	0.994	0.964	0.886	0.994	0.994	0.991	0.958	0.967	0.927	0.927		0.003	0.002	0.003	0.007	0.019
12 *Parabistichella cystiformans* KJ509196	0.960	0.954	0.917	0.959	0.960	0.958	0.991	0.988	0.959	0.959	0.960		0.002	0.003	0.008	0.020
13 *Lamtostyla ovalis* KP266625	0.995	0.965	0.886	0.994	0.995	0.993	0.958	0.967	0.927	0.927	0.995	0.963		0.003	0.008	0.019
14 *Parabistichella dieckmanni* MN994505	0.974	0.968	0.902	0.973	0.976	0.974	0.974	0.983	0.944	0.942	0.976	0.978	0.976		0.005	0.018
15 *Paraholosticha muscicola* KT003281	0.894	0.922	0.975	0.894	0.896	0.894	0.930	0.923	0.938	0.938	0.896	0.926	0.895	0.915		0.018
16 *Pseudokahliella marina* KM222095	0.976	0.946	0.870	0.976	0.979	0.978	0.941	0.949	0.910	0.909	0.978	0.943	0.978	0.962	0.886	

Discussion

Morphological comparison with congeners (Table 3)

Table 3 Morphological comparison of *Bistichella granulifera* n. sp. with its congeners.

Characteristic	*B. granulifera* n. sp.	*B. buitkampi*	*B. chilensis*	*B. humicola*	*B. kenyaensis*
Body shape	Elongated oval	Slightly dumbbell-shaped to sigmoidal	Slenderly ellipsoid to almost rectangular	Elongate ellipsoid with margins converging posteriorly	Ellipsoid to slenderly ellipsoid, but usually widest anterior of mid-body
Cortical granules	Present	Absent	Absent	N/A	Absent
Adoral membranelles, number	33–38	34–40	25–38	31	21–30
Frontal cirri, number	3	3	4	3	3
Buccal cirri, number	3 or 4	2–4	4–6	1	2 or 3
Frontal rows, number	3	1 or 2	2 or 3	1	2 or 3
Frontal rows, number of cirri	7-10	2-10	6-13	9	4-6
Termination of frontoventral row I	90% down length of body	75% down length of body	76% down length of body	64% down length of body	54% down length of body
Frontoventral row I, number of cirri	26–37	25–37	16–33	24*	9–20
Frontoventral row II	Not interrupted	Interrupted	Interrupted	Not interrupted	Interrupted
Right marginal row, number of cirri	48–54	39–49	29–55	41	30–43
Macronuclear nodules, number	2	4	2 or 3	32	2
Data source	Present study	Foissner (1982) Berger (2008)	Foissner (2016)	Gellért (1956) Berger (2008)	Foissner (2016)

* Data from illustration.
a Body size may be measured after fixation.
b A short cirral row included, which located in rear body portion.

Our new isolate matches *Bistichella* in almost all key features, i.e. three or four frontal cirri, two or three short frontal and two or three frontoventral rows, and more than one buccal cirrus, transverse cirri absent, dorsal kinety pattern of *Gonostomum*-type, etc. Up to now, four valid species of *Bistichella* are recognized, namely, *B. buitkampi*, *B. humicola*, *B. chilensis* and *B. kenyaensis* [1, 4, 15, 16].

Compared to the type species, *Bistichella buitkampi*, *B. granulifera* n. sp. can be distinguished by having more frontal rows (three vs. one or two), less macronuclear nodules (two vs. four), longer frontoventral row I (terminates at 90% vs. 75% down length of body) and cortical granules present (vs. absent). Note that, in *B. buitkampi*, a short longitudinal cirral row in the rear portion of the body was termed transverse cirri in the original description [1, 15].

In terms of the infraciliature, *Bistichella chilensis* is closely related to *B. granulifera* n. sp. The former can be recognized by having body shape slenderly ellipsoid to almost rectangular (vs. elongated oval), four (vs. three) frontal cirri, a wide break in the right frontoventral row at mid-body (vs. no break), termination of frontoventral row I at 76% (vs. 90%) down length of body and cortical granules absent (vs. present) [4].

Even though the morphology of *Bistichella humicola* is not very detailed, given present knowledge, *B. granulifera* n. sp. can be easily separated with *B. humicola* by having not tapered tail (vs. slightly tapered), three or four (vs. only one) buccal cirri and three (vs. one)

frontal rows, lower termination of frontoventral row I (90% vs. 64% down length of body) and less (two vs. 32) macronuclear nodules [1, 16].

Bistichella kenyaensis differs from the *B. granulifera* n. sp. by having body shape ellipsoid to slenderly ellipsoid, and usually widest anterior of mid-body (vs. elongated oval and widest at mid-body), the right frontoventral row with a very wide break in the middle quarters of body (vs. no break), fewer adoral membranelles (21–30 vs. 33–38) and cirri in the frontal rows (4–6 vs.7–10), frontoventral row I (9–20 vs. 26–37) and right marginal row (30–43 vs. 48–54), shorter frontoventral row I (terminates at 54% vs. 90% down length of body) and no cortical granules (vs. present) [4].

Morphogenetic comparison

The morphogenesis of *Bistichella* species is reported for the first time in present work. Based on the investigation, the main characteristic events during morphogenesis of the *B. granulifera* n. sp. can be summarized as follows: (1) in the proter, the posterior part of the parental AZM is renewed; in the opisthe; (2) frontoventral-transverse cirral anlagen III to V each form a frontal row and anlagen VI to n each produces a frontoventral row; (3) the left and right marginal anlagen develop intrakinetally; (4) dorsal morphogenesis follows a typical *Gonostomum*-pattern; and (5) the macronuclear nodules fuse to form a single mass.

The genus *Parabistichella* resembles *Bistichella* in terms of forming a row of buccal cirri, marginal anlagen and dorsal kineties anlagen developing intrakinetally [1, 4, 19–22]. However, *Bistichella* can be distinguished by a lack of transverse cirri (vs. formed in *Parabistichella*) [4, 19, 21]. Another important morphogenetic feature is the origin of the frontoventral row. Hitherto, in *Parabistichella*, morphogenetic data is available for only three species, which are *P. variabilis*, *P. cystiformans* and *P. dieckmanni*. However, each frontoventral row is produced by one anlage in *P. cystiformans*, whereas the left frontoventral row originating from two anlagen in *P. dieckmanni* (morphogenesis is described very roughly in the type species, *P. variabilis*, so data unavailable) [10, 19, 21, 22]. *B. granulifera* n. sp. shows similarity to *P. cystiformans* in that the frontoventral row originates from one anlage.

Phylogenetic analyses

Berger (2008) [1] classified *Bistichella* as *incertae sedis* in Hypotrichia. In the phylogenetic tree, *Bistichella* has a close relationship with stichotrichids (Fig. 5). Additionally, *Bistichella* falls into a clade which includes *Uroleptoides*, *Parabistichella*, *Orthoamphisiella*, *Lamtostyla*, *Keronopsis*, *Paraholosticha* and *Pseudokahliella*, and shares the same morphological features, i.e., at least one long or moderate long frontoventral row, one marginal cirral row on each side, constantly three bipolar dorsal kineties, and a lack of dorsomarginal kineties. They are all non-dorsomarginalian hypotrichs, and this clade is separate with Dorsomarginalia, all species of which have dorsomarginal row [1, 19, 21, 23–29]. The result further proves the importance of dorsal structure in hypotrichous classification.

The sequence of the type species, *B. buitkampi*, is still unknown. Even though the phylogenetic position of *B. granulifera* n. sp. was shown in present work, the position of the genus *Bistichella* cannot be certain. Futhermore, only a few sequences of genera, which are morphological similar with *Bistichella* (*Lamtostyla*, *Orthoamphisiella* and *Uroleptoides*), are available, and the bootstrap values are very low in the phylogenetic tree, which is also seen previous work [22, 30–32]. Therefore, we cannot reach a conclusion of the phylogenetic relationship between *Bistichella* and its morphological similar genera. Further investigations with additional taxa and molecular data may reveal the evolution of *Bistichella*.

Conclusions

The morphology, morphogenesis and phylogeny of *Bistichella granulifera* n. sp. is described. In the phylogenetic tree, *B. granulifera* n. sp. has a close relationship with species which have three bipolar dorsal kineties, and a lack of dorsomarginal kineties. Therefore, *Bistichella* should belong to non-Dorsomarginalia. Also, further morphogenetic and molecular studies would help to confirm the phylogenetic position of *Bistichella*.

Methods

Sampling and cultivation

Bistichella granulifera n. sp. was isolated from a soil sample which was collected on 17 April 2016 from a hill in Jiangjunshan ancient town (34º02'16"N; 109º04'53"E), Xi'an, China. Ciliates were stimulated to excyst and emerge from the soil sample using the non-flooded Petri dish method [18]. Cells were maintained in the raw cultures at room temperature (about 24°C) using sterile water, with bacteria and mainly small ciliates as food sources. However, only a low number of cells were found. A clonal culture could not be established in the laboratory. The species was accurately identified based on its morphological and morphogenetic characteristics. Moreover, no other *Bistichella* specimens were present in the protargol preparations. Therefore, it is almost certain that all data is based on *B. granulifera* n. sp.

Morphology and morphogenesis

Living cells were observed using bright field and differential interference contrast microscopy (Olympus BX52), and specimens were photographed using a digital camera. The protargol method was used to reveal the ciliature and the nuclear apparatus [33]. Counts and measurements of stained specimens were performed at a magnification of 1,000×. Drawings of stained cells were made with the aid of a camera lucida. To illustrate the changes occurring during morphogenesis process, ciliary structures of parental cirri and membranelles are depicted by contour lines, whereas new ones are shaded black [34]. Terminology is according to Berger (2008) [1].

DNA extraction, PCR amplification, and sequencing

A few cells of *Bistichella granulifera* n. sp. were isolated and repeatedly washed with sterilized distilled water. Genomic DNA was extracted from cells using DNeasy Blood & Tissue Kit (Qiagen, CA) following the manufacturer's instructions. The SSU rDNA was amplified using the eukaryotic universal primers 18S-F and 18S-R [35]. The amplification cycles were according to previous work [36, 37]. High-fidelity Taq polymerase (Takara Ex Taq, Takara Biomedicals) was used to minimize the possibility of amplification errors. Sequencing of the PCR products was performed bidirectionally on an ABI 3700 sequencer (Invitrogen sequencing facility, Shanghai, China) using primers 18S-F, 18S-R and three internal primers 900F, 900R and Pro B [37].

Phylogenetic analyses

The SSU rDNA sequence of the *Bistichella granulifera* n. sp. was aligned with sequences of 70 representative taxa downloaded from the GenBank database. Four species were selected as the outgroup species. The accession number of each species is mentioned in the phylogenetic tree (Fig. 5). Subsequently, all sequences were aligned using the GUIDANCE web server (http://guidance.tau.ac.il/) [38]. The resulting alignment was manually edited using the program BioEdit 7.0, which removed ambiguous regions and trimmed the ends [39]. Maximum likelihood (ML) analyses were performed online using RAxML-HPC2 on XSEDE v8.2.9 [40, 41] on the CIPRES Science Gateway [42]. The reliability of internal branches was assessed using a nonparametric bootstrap method with 1000 replicates. Bayesian inference (BI) was performed using MrBayes on XSEDE 3.2.6 [43] with the best-fit model GTR + I + G model as selected by Akaike Information Criterion (AIC) in MrModeltest v.2.0 [44]. Markov chain Monte Carlo simulations were run for 1 000 000 generations with a sampling frequency of 100 and a burn-in of 1000 trees. The remaining trees were used to calculate the posterior probabilities (PP) with a majority rule consensus. SeaView v.4 [45] and MEGA v7.0 [46] were used to visualize the tree topologies.

Abbreviations

AZM: adoral zone of membranelles; BI: Bayesian inference; bp: base pairs; GC: Guanine-cytosine; ML: Maximum likelihood; n. sp.: novum species; PCR: Polymerase chain reaction; SSU rDNA: Small subunit ribosomal DNA.

Declarations

Ethics approval and consent to participate

Not applicable.

Consent for publication

Not applicable.

Availability of data and materials

Sequence data are available in GenBank (Accession Numbers: MT604042). Three protargol slides have been deposited in the collection of the Laboratory of Protozoological Biodiversity and Evolution in Wetland, Shaanxi Normal University, China (accession numbers: LZ2016041701A–C).

Competing interests

The authors declare that they have no competing interests.

Funding

This work was financially supported by the Natural Science Foundation of China (Project number: 31872190). The funding bodies had no role in the design or implementation of this study or in preparation of the manuscript.

Authors' contributions

LZ collected the samples, did protargol preparations, and wrote the main part of the manuscript; LJ analyzed data and wrote some parts of the manuscript; WY extracted DNA and built the phylogenetic tree; MJ depicted infraciliature and provided the morphometric data; SC conducted the experiment and revised the manuscript. All the authors checked the manuscript before submission.

Acknowledgements

Many thanks are given to Mr. Dale Oyston for correcting the English of this paper.

References

1. Berger H. Monograph of the Amphisiellidae and Trachelostylidae (Ciliophora, Hypotricha). Monogr 2008;88:1–737.
2. Berger H. Monograph of the Gonostomatidae and Kahliellidae (Ciliophora, Hypotricha). Monogr Biol. 2011;90:1–741.
3. Bhartia D, Kumar S, Terza AL, Chandra K. Morphology and ontogeny of *Tetmemena pustulata indica* subspec. (Ciliophora, Hypotricha), from the Thane Creek, Mumbai, India. Eur J Protistol. 2019;71:125629.
4. Foissner W. Terrestrial and semiterrestrial ciliates (Protozoa, Ciliophora) from Venezuela and Galápagos. Denisia 2016;35:487–
5. Hu X, Lin X. Song W. Ciliates Atlas: Species Found in the South China Sea. Science Press (Beijing) 2019;p:1–
6. Luo X, Huang J, Li L, Song W, Bourland WA. Phylogeny of the ciliate family Psilotrichidae (Protista, Ciliophora), a curious and poorly-known taxon, with notes on two algae-bearing psilotrichids from Guam, USA. BMC Evolut Biol. 2019;19:125.
7. Song W, Shao C. Ontogenetic Patterns of Hypotrich Ciliates. Science Press (in Chinese). 2017;p:1–
8. Zhang T, Dong J, Cheng T, Duan L, Shao C. Reconsideration of the taxonomy of the marine ciliate *Neobakuella aenigmatica* Moon et al., 2019 (Protozoa, Ciliophora, Hypotrichia). Mar Life Sci Technol. 2020;2:97–
9. Chen L, Dong J, Wu W, Xin Y, Warren A, Ning Y, Zhao Y. Morphology and molecular phylogeny of a new hypotrich ciliate, *Anteholosticha songi* spec., and an American population of *Holosticha pullaster* (Müller, 1773) Foissner et al., 1991 (Ciliophora, Hypotrichia). Eur J Protistol. 2020;72:125646.
10. Dong J, Chen X, Liu Y, Ni B, Fan X, Li L, Warren A. An integrative investigation of *Parabistichella variabilis* (Protista, Ciliophora, Hypotrichia) including its general morphology, ultrastructure, ontogenesis, and molecular phylogeny. J Eukaryot Microbiol. 2020;doi:10.1111/jeu.12809.
11. Kaur H, Shashi, Negi RK, Kamra K. Morphological and molecular characterization of *Neogastrostyla aqua* gen., nov. spec. (Ciliophora, Hypotrichia) from River Yamuna, Delhi; comparison with *Gastrostyla*-like genera. Eur J Protistol. 2019;68:68–79.
12. Kim KS, Min GS. Morphology and molecular phylogeny of *Oxytricha seokmoensis* nov. (Hypotrichia: Oxytrichidae), with notes on its morphogenesis. Eur J Protistol. 2019;71:125641.
13. Jung JH., Berger H. Monographic treatment of *Paraholosticha muscicola* (Ciliophora, Keronopsidae), including morphological and molecular biological characterization of a brackish water population from Korea. Eur J Protistol. 2019;68:48–
14. Park KM, Jung JH, Jeong HK, Min GS, Kim S. Morphology, morphogenesis, and molecular phylogeny of a new freshwater ciliate, *Gonostomum jangbogoensis* sp. (Ciliophora, Hypotricha), from Victoria Land, Antarctica. Eur J Protistol. 2020;73:125669.

15. Foissner W. Ökologie und Taxonomie der Hypotrichida (Protozoa: Ciliophora) einiger österreichischer Böden). Archiv Für Protistenkind 1982;126:19–143.
16. Gellért J. Ciliaten des sic hunter dem Moosrasen auf Felsen gebildeten Humus. Acta Biol Hung 1956;6, 337–359.
17. Aescht E. Annotated catalogue of “type material” of ciliates (Ciliophora) and some further protists at the Upper Austrian Museum in Linz (Austria) including a guideline for “typification” of species. Denisia 2008;23:125–234.
18. Foissner W. An update of ‘basic light and scanning electron microscopic methods for taxonomic studies of ciliated protozoa’. Int J Syst Evol Microbiol. 2014;64:271–
19. Fan Y, Hu X, Gao F, Al-Farraj SA, Al-Rasheid KAS. Morphology, ontogenetic features and SSU rRNA gene-based phylogeny of a soil ciliate, *Bistichella cystiformans* nov. (Protista, Ciliophora, Stichotrichia). Int J Syst Evol Microbiol. 2014;64:4049–4060.
20. He Y, Xu K. Morphology and small subunit rDNA phylogeny of a new soil ciliate, *Bistichella variabilis* sp. (Ciliophora, Stichotrichia). J Eukaryot Microbiol. 2011;58:332–338.
21. Jiang J, Huang J, Li L, Shao C, Al-Rasheid KAS, Al-Farraj SA, Chen Z. Morphology, ontogeny, and molecular phylogeny of two novel bakuellid-like hypotrichs (Ciliophora: Hypotrichia), with establishment of two new genera. Eur J Protistol. 2013;49:78–92.
22. Lyu Z, Li J, Shao C. Redescription of the soil hypotrichous ciliate, *Parabistichella dieckmanni* (Foissner, 1998) Foissner, 2016 (Ciliophora, Hypotrichia), with notes on its morphogenesis and phylogeny. J Eukaryot Microbiol. 2020;
23. Dong J, Li L, Fan X, Ma H, Warren A. 2020. Two *Urosoma* species (Ciliophora, Hypotrichia): A multidisciplinary approach provides new insights into their ultrastructure and systematics. Eur J Protistol. 2020;72:125661.
24. Lu X, Wang Y, Al-Farraj SA, El-Serehy H, Huang J, Shao C. The insights into the systematic relationship of *Gastrostyla*-affinitive genera, with report on a new saline soil ciliate genus and new species (Protozoa, Ciliophora). BMC Evolut Biol. 2020;in press.
25. Luo X, Yi Z, Gao F, Pan Y, Al-Farraj SA, Warren A. Taxonomy and molecular phylogeny of two new brackish hypotrichous ciliates, with the establishment of a new genus (Protozoa, Ciliophora). Zool J Linn Soc. 2016;179:475–491
26. Ma J, Zhao Y, Zhang T, Shao C, Al-Rasheid KAS, Song W. Cell-division pattern and phylogenetic analyses of a new ciliate genus *Parasincirra* g. (Protista, Ciliophora, Hypotrichia), with a report of a new soil species, *P. sinica* n. sp. from northwest China BMC Evolut Biol. 2020;in press.
27. Shao C, Hu C, Fan Y, Warren A, Lin X. Morphology, morphogenesis and molecular phylogeny of a freshwater ciliate, *Monomicrocaryon euglenivorum euglenivorum* (Ciliophora, Oxytrichidae). Eur J Protistol. 2019;68:25–36.
28. Wang J, Li J, Qi S, Warren A, Shao C. Morphogenesis and molecular phylogeny of a soil ciliate *Uroleptoides longiseries* (Foissner, Agatha and Berger, 2002) Berger, 2008 (Ciliophora, Hypotrichia). J Eukaryot Microbiol. 2019;66:334–342.
29. Xu W, Zhao Y, Pan B, Liu Y, Li Y, Bourland, WA, Luo X. 2020. Morphology, morphogenesis, and phylogeny of *Urosoma caudata* (Ehrenberg, 1833) Berger, 1999 (Ciliophora, Hypotrichia) based on a Chinese population. J Eukaryot Microbiol. 2020;67:76–85.
30. Luo X, Yan Y, Shao C, Al-Farraj SA, Bourland WA, Song W. Morphological, ontogenetic and molecular data support strongylidiids as being closely related to Dorsomarginalia (Protozoa, Ciliophora) and reactivation of the family Strongylidiidae Fauré-Fremiet, 1961. Zool J Linn Soc. 2018;184:237–
31. Park KM, Chae N, Jung JH, Min GS, Kim S, Berger H. Redescription of *Keronopsis helluo* Penard, 1922 from Antarctica and *Paraholosticha pannonica* Gellért and Tamás, 1959 from Alaska (Ciliophora, Hypotricha). Eur J Protistol. 2017;60:102–118.
32. Dong J, Lu X, Shao C, Huang J, Al-Rasheid KA. S. Morphology, morphogenesis and molecular phylogeny of a novel saline soil ciliate, *Lamtostyla salina* sp. (Ciliophora, Hypotricha). Eur J Protistol. 2016;56:219–231.
33. Wilbert N. Eine verbesserte technik der Protargolimprägnation für ciliaten. Mikrokosmos 1975;64:171–179.
34. Wang J, Li J, Shao C. Morphology, morphogenesis, and molecular phylogeny of a novel saline soil ciliate, *Heterourosomoida sinica* sp. (Ciliophora, Hypotrichia). Eur J Protistol. 2020;73:125666.
35. Medlin L, Elwood HJ, Stickel S, Sogin ML. The characterization of enzymatically amplified eukaryotic 16S-like rRNA-coding regions. Gene 1988;71:491–499.
36. Lyu Z, Wang J, Huang J, Warren A, Shao C. Multigenebased phylogeny of Urostylida (Ciliophora, Hypotrichia), with establishment of a novel family. Zool Scr. 2018;47:243–254.
37. Wang J, Zhao Y, Lu X, Lyu Z, Warren A, Shao C. Does the *Gonostomum*-patterned oral apparatus in hypotrichia carry a phylogenetic signal? Evidence from morphological and molecular data based on extended taxon sampling using three nuclear genes (Ciliophora, Spirotrichea). Sci China Life Sci. 2020;63:https://doi.org/10.1007/s11427-020-1667-3.

38. Penn O, Privman E, Ashkenazy H, Landan G, Graur D, Pupko T. GUIDANCE: a web server for assessing alignment confidence scores. Nucleic Acids Res. 2010;38:W23–W28.
39. Hall TA. BioEdit: a user-friendly biological sequence alignment editor and analysis program for Windows 95/98/NT. Acids Symp Ser. 1999;41:95–98.
40. Stamatakis A. RAxML version 8: a tool for phylogenetic analysis and post-analysis of large phylogenies. Bioinformatics 2014;30:1312–1313.
41. Stamatakis A, Hoover P, Rougemont J. A rapid bootstrap algorithm for the RAxML web-servers. Syst Biol. 2008;57:758–771.
42. Miller MA, Pfeiffer W, Schwartz T. Creating the CIPRES science gateway for inference of large phylogenetic trees. In: Proceedings of the Gateway Computing Environments Workshop (GCE), New Orleans, LA. 2010;1–8. https://doi.org/10.1109/GCE.2010.5676129.
43. Ronquist F, Teslenko M., van der Mark P, Ayres DL, Darling A, Höhna S, Larget B, Liu L, Suchard MA, Huelsenbeck JP. MrBayes 3.2: efficient Bayesian phylogenetic inference and model choice across a large model space. Syst Biol. 2012;61:539–542.
44. Nylander JAA. 2004. MrModeltest, Version 2.2. Program distributed by the author. Evolutionary Biology Centre, Uppsala University,
45. Gouy M, Guindon S, Gascuel O. SeaView version 4: a multiplatform graphical user interface for sequence alignment and phylogenetic tree building. Mol Biol Evol. 2010;27:221–224.
46. Tamura K, Peterson D, Peterson N, Stecher G, Nei M, Kumar S. MEGA5: molecular evolutionary genetics analysis using maximum likelihood, evolutionary distance, and maximum parsimony methods. Mol Biol Evol, 2011;28:2731–2739.

Figures

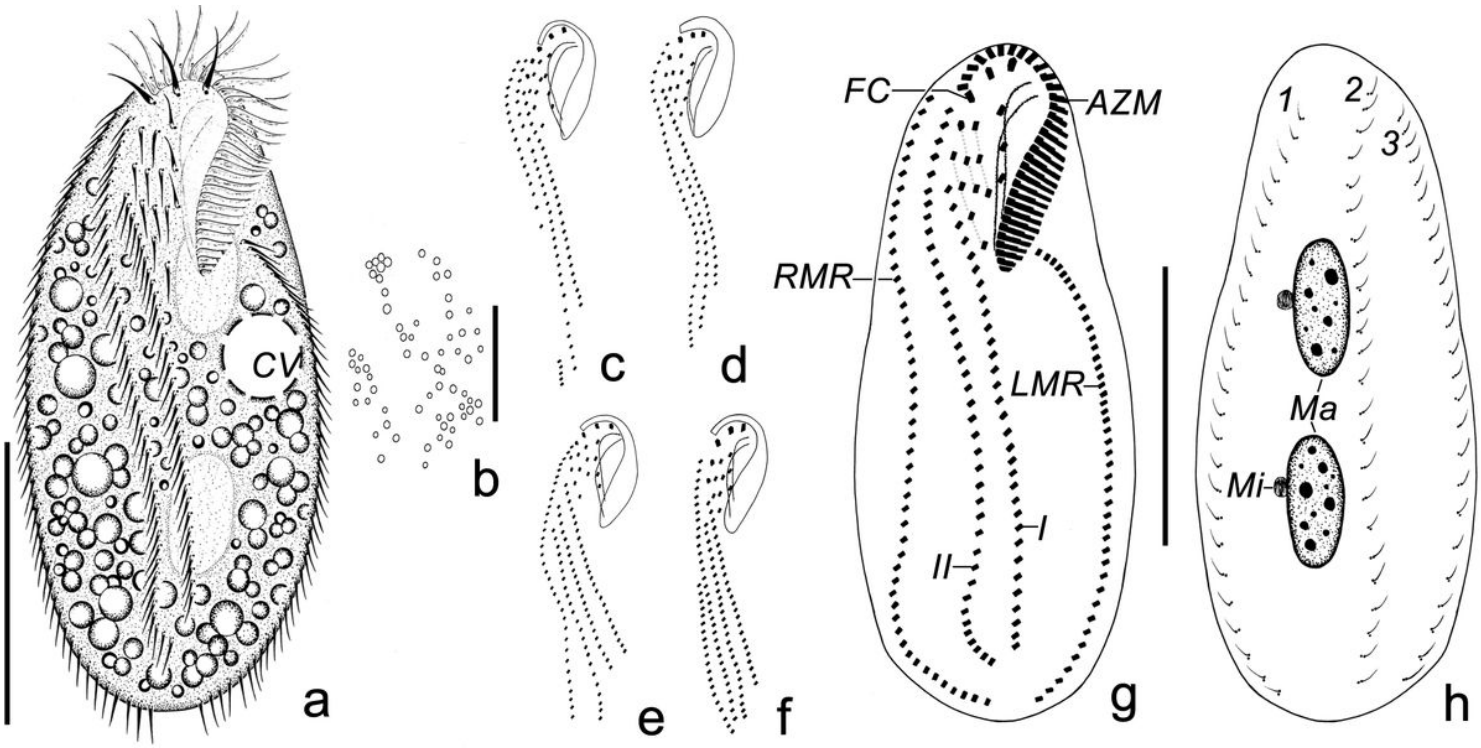

Figure 1

a–h. Morphology of Bistichella granulifera n. sp. from life (a) and after protargol staining (b–g). (a) Ventral view of a representative individual. (b–e) Ventral views of some other specimens to show the variety in the infraciliature. (f, g) Ventral (f) and dorsal (g) view of the holotype to show the infraciliature and nuclear apparatus. Dotted lines connect cirri in frontal rows. AZM, adoral zone of membranelles; FC, frontal cirri; LMR, left marginal row; Ma, macronuclear nodules; Mi, micronuclei; RMR, right marginal row; I, II, frontoventral rows I and II; 1–3, dorsal kineties. Scale bars = 50 μm (a, g, h); 10 μm (b).

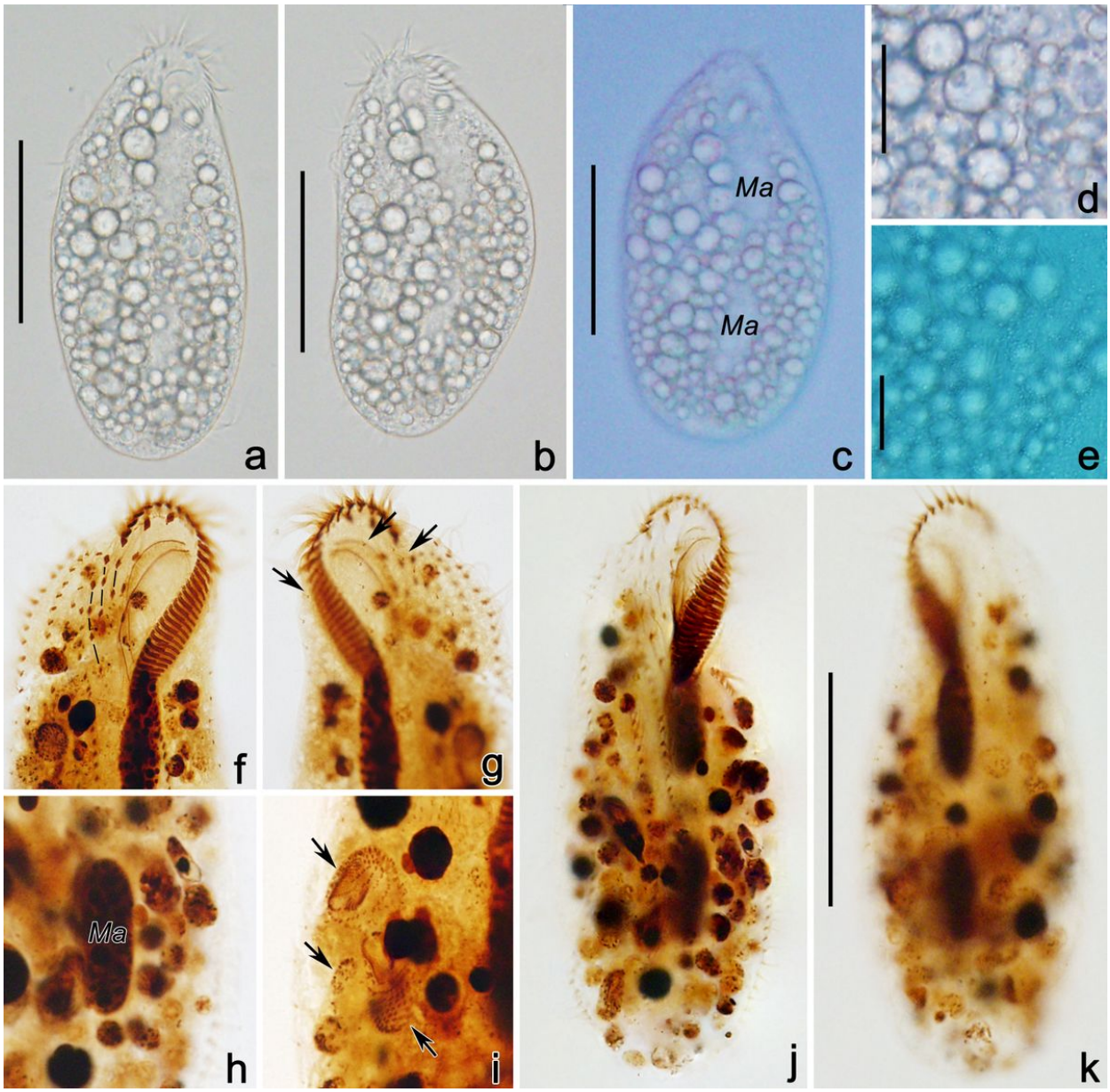

Figure 2

a–k. Microphotographs of Bistichella granulifera n. sp. from life (a–e) and after protargol impregnation (f–k). (a–c) Ventral views of typical individuals, showing the different body shapes. (d) Cytoplasm with many food vacuoles and lipid droplets. (e) Cortical granules densely scattered throughout cell surface. (f) Ventral view of the anterior portion, dash lines show three short frontal cirral rows. (g) Dorsal view of the anterior portion, arrows demonstrate three dorsal kineties. (h) Macronuclear nodule. (i) Some small ingested ciliate (arrows). (j, k) Ventral (j) and dorsal (k) view of holotype specimen, showing infraciliature and nuclear apparatus. Scale bars = 50 μm (a–c, j, k); 10 μm (d, e).

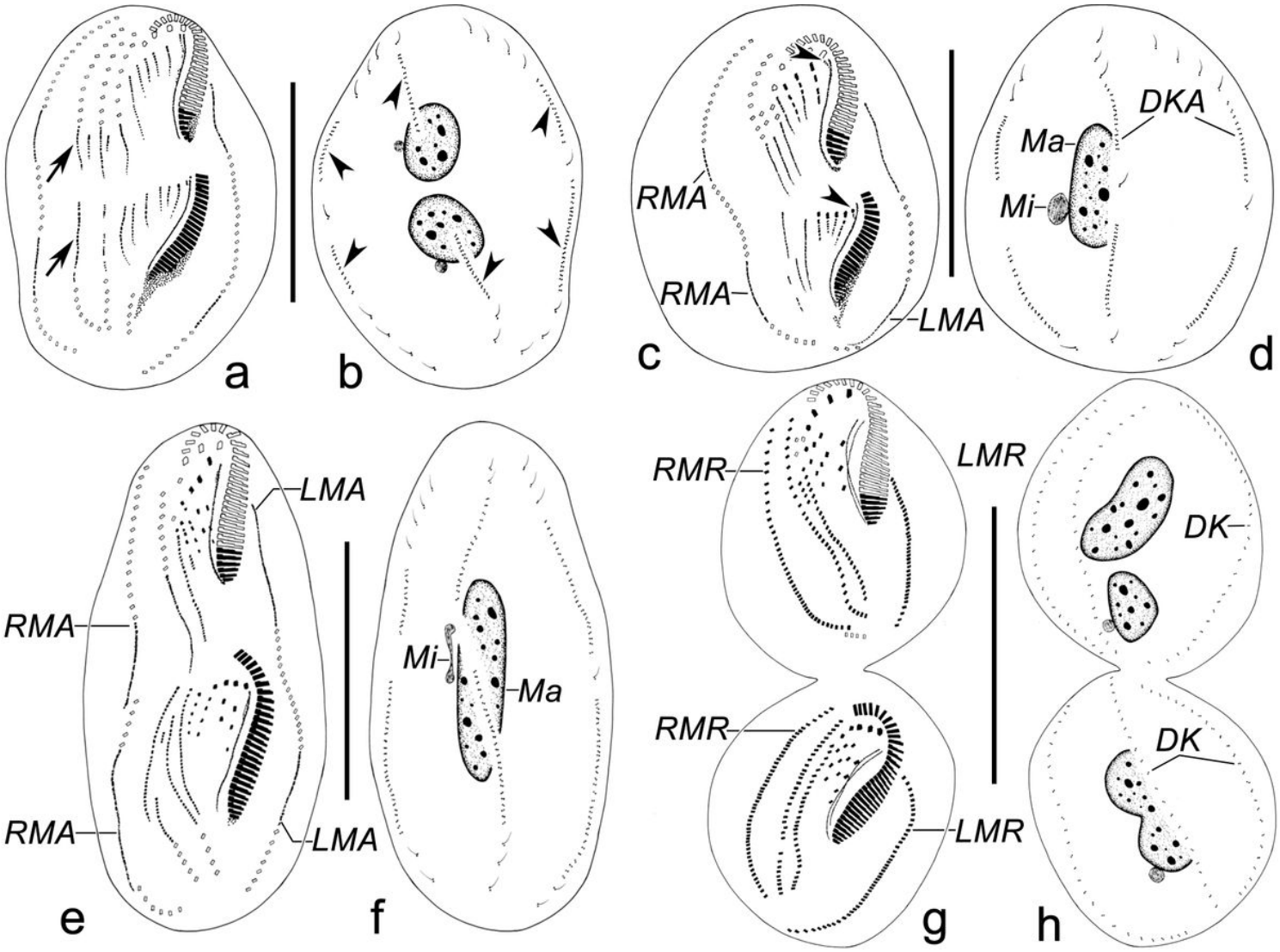

Figure 3

a–h. Morphogenesis of Bistichella granulifera n. sp. after protargol staining. (a, b) Ventral and dorsal view of an early divider, showing the formation of the frontoventral-transverse cirral anlagen (arrows). Note the proximal end of the old adoral zone of membranelles dedifferentiate and form the new membranelle, as well as marginal and dorsal kineties anlagen (arrowheads in b) develop intrakinetally. (c, d) Ventral and dorsal view of a middle divider, depicting formation of the leftmost frontal cirri (arrowheads), frontoventral-transverse cirral anlagen beginning to differentiate into cirri, and macronuclear nodules fused into a single mass. (e, f) Ventral and dorsal view of a middle divider, to demonstrate anlagen differentiated into cirri, the new adoral membranelles completed in the opisthe, and micronuclei divide mitotically. (g, h) Ventral and dorsal view of a late divider, marking the new cirri migrating into their final positions, undulating membranes anlagen longitudinally splitting into parorals and endorals, and the macronuclear nodules divided. DK, dorsal kineties; DKA, dorsal kineties anlagen; LMA, left marginal anlage; LMR, left marginal row; Ma, macronuclear nodules; Mi, micronuclei; RMA, right marginal anlage; RMR, right marginal row. Scale bars = 80 μm.

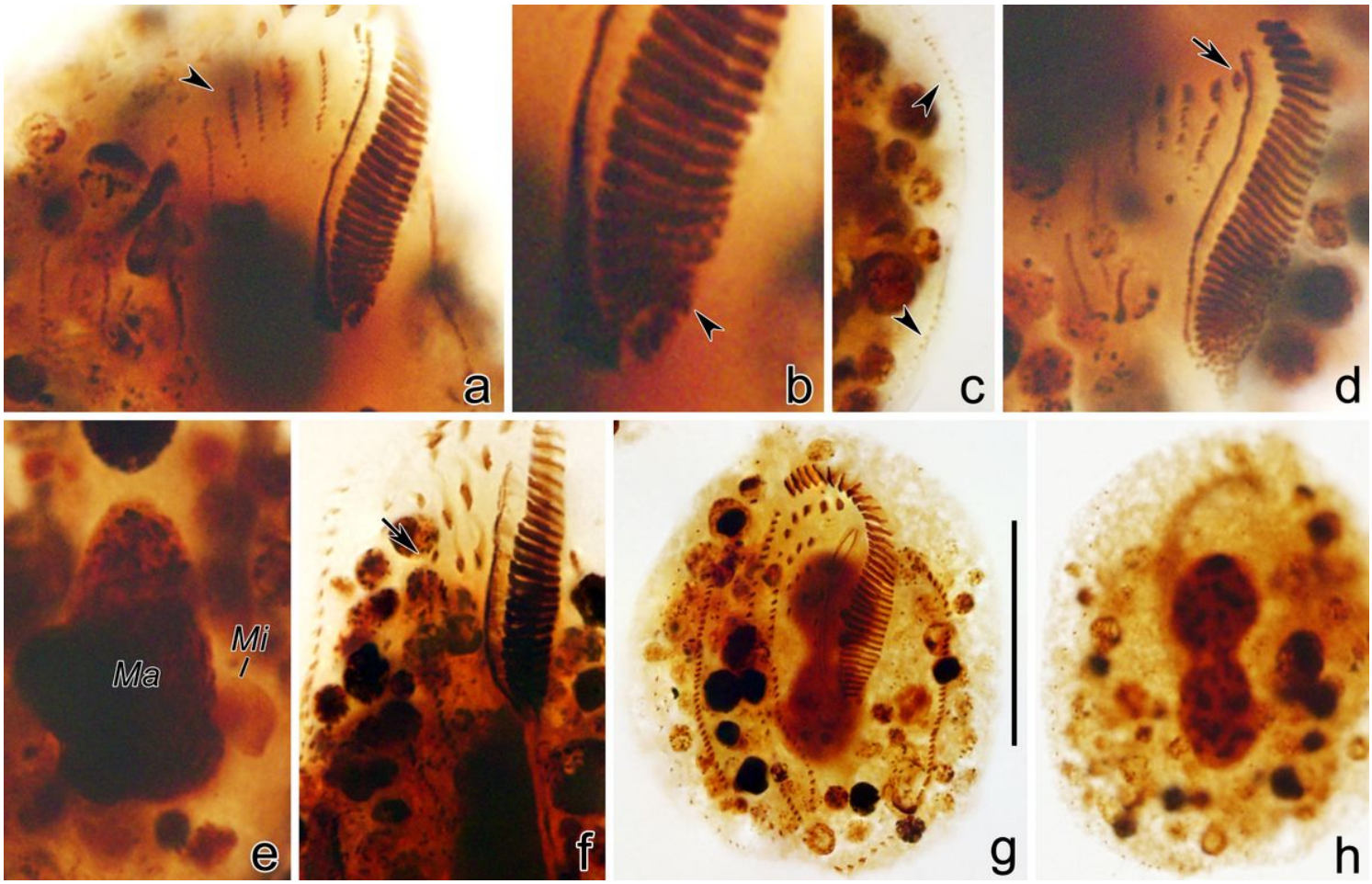

Figure 4

a–h. Photomicrographs of Bistichella granulifera n. sp. during morphogenesis after protargol staining (a–h). (a) Ventral view of an early divider to show the frontoventral-transverse cirral anlagen formed (arrowhead). (b) The old adoral zone of membranelles start to dedifferentiate and form the new membranelles (arrowhead). (c) Dorsal kineties develop intrakinetally (arrowheads). (d) Ventral view of a middle divider, showing that the first frontal cirrus originates from the undulating membranes anlage (arrow), the frontoventral-transverse cirral anlagen differentiate into cirri and the new adoral membranelles differentiate posteriad in the opisthe. (e) Macronuclear nodules fuse into a single mass. (f) Ventral view of a middle divider demonstrating the almost completed segmentation of the frontoventral-transverse cirral anlagen (arrow). (g, h) Ventral and dorsal view of a late divider, to depict cirri migrating into their final positions. Ma, macronuclear nodules; Mi, micronuclei. Scale bars = 30 μm.

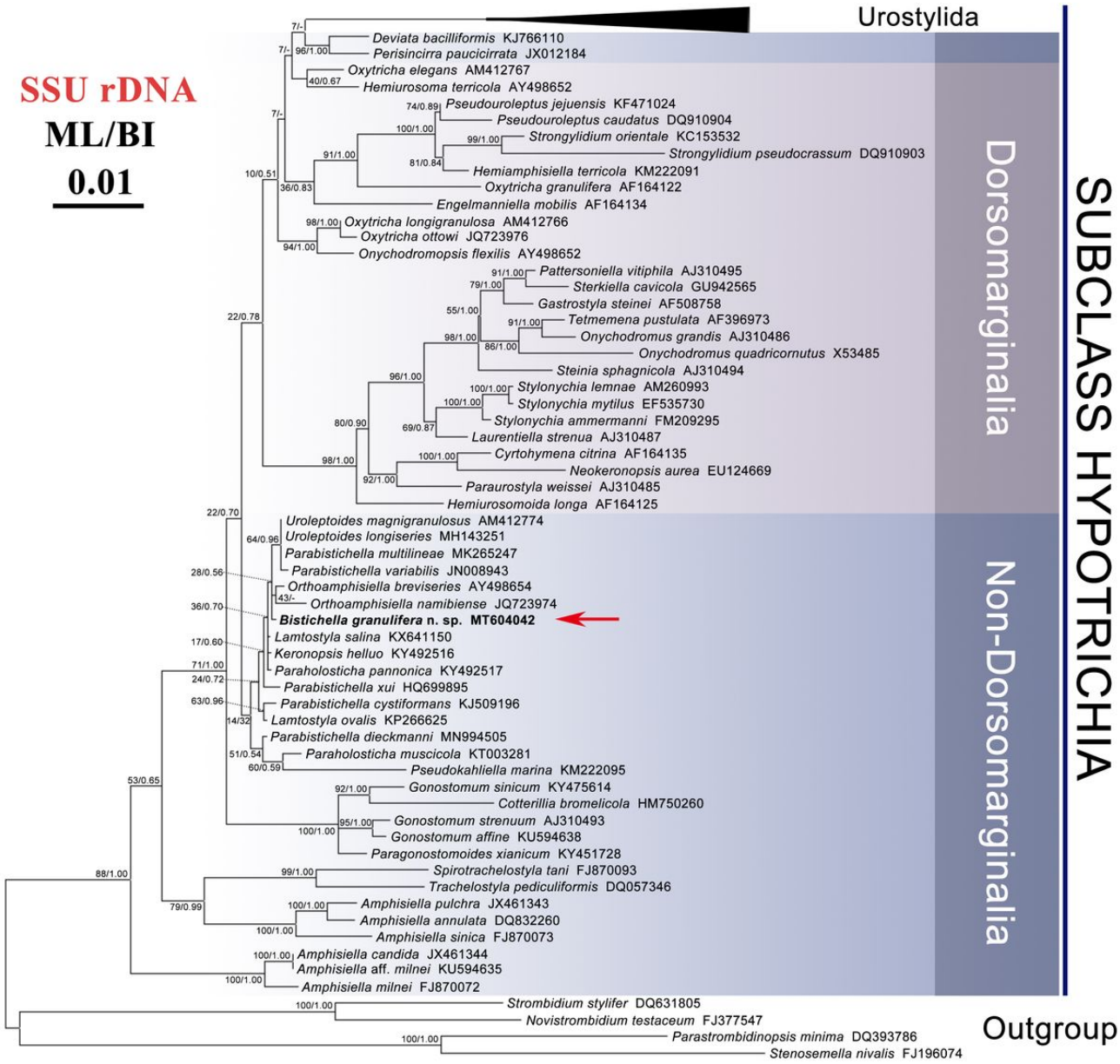

Figure 5

Maximum likelihood (ML) tree inferred from the SSU rDNA sequences showing the systematic position of Bistichella granulifera n. sp. (in bold). Numbers near nodes are bootstrap values for maximum-likelihood and posterior probability values for Bayesian inference (BI). "-" at nodes indicate disagreement between the two methods. The scale bar corresponds to 0.01 expected substitutions per site.